

Synthesis and Evaluation of the Anti-Inflammatory Activity of the Schiff Base Ligand (2-(1H-Benzo[d]imidazol-2-Yl)phenol) and Its Co(II) and Mn(III) Complexes

Ngoné Diouf¹, Awa Ndiaye Sy^{2*}, Nango Gaye¹, Idrissa Ndoye³, Diatta Charlot², Adama Diédhiou³, Mamadou Baldé³, Sène Madièye², Birame Faye², Yoro Tine³, Djibril Fall³, Alassane Wélé³, Thiam Elhadj Ibrahima¹, Rokhaya Sylla Guèye³

¹Department of Chemistry, Faculty of Science and Technology, Cheikh Anta Diop University of Dakar, Dakar, Senegal

²Laboratory of Pharmacology and Pharmacodynamics, Faculty of Medicine, Pharmacy, and Odonto-Stomatology, Cheikh Anta Diop University of Dakar, Dakar, Sénégal

³Laboratory of Organic and Therapeutic Chemistry, Faculty of Medicine, Pharmacy, and Odonto-Stomatology, Cheikh Anta Diop University of Dakar, Dakar, Senegal

Email: *awa.sy@ucad.edu.sn

How to cite this paper: Diouf, N., Sy, A.N., Gaye, N., Ndoye, I., Charlot, D., Diédhiou, A., Baldé, M., Madièye, S., Faye, B., Tine, Y., Fall, D., Wélé, A., Ibrahima, T.E. and Guèye, R.S. (2026) Synthesis and Evaluation of the Anti-Inflammatory Activity of the Schiff Base Ligand (2-(1H-Benzo[d]imidazol-2-Yl)phenol) and Its Co(II) and Mn(III) Complexes. *Pharmacology & Pharmacy*, 17, 142-154.

<https://doi.org/10.4236/pp.2026.172007>

Received: January 16, 2026

Accepted: February 25, 2026

Published: February 28, 2026

Copyright © 2026 by author(s) and Scientific Research Publishing Inc.

This work is licensed under the Creative Commons Attribution International License (CC BY 4.0).

<http://creativecommons.org/licenses/by/4.0/>



Open Access

Abstract

Coordination complexes are inorganic compounds that play an important role in medicinal chemistry. They possess numerous properties such as denticity, flexibility, reactivity, and stability. Schiff base ligands are organic compounds obtained from the condensation reaction between a carbonyl compound and a primary amine. They are used in many fields, including analytical, biological, organic, and inorganic industries. In this context, we synthesized a Schiff base ligand as well as two dinuclear complexes of cobalt and manganese. Various techniques such as IR, 1H and 13C NMR, UV-visible, conductimetry, magnetism, and XRD were used to characterize these compounds. The local anti-inflammatory activity of these compounds and the reference indomethacin was evaluated in mice by measuring the inflammatory response to the topical application of an irritant (croton oil) to the ear. The results of the comparative study of the anti-inflammatory properties of the free ligand and its complexes led to the conclusion that the complexes are more active than the ligand.

Keywords

Schiff Bases, Complexes, Cobalt, Manganese, Anti-Inflammatory Activity

1. Introduction

Inflammation is a physiological response to injury and infectious, allergic, or chemical irritation. It can maintain, induce, or aggravate many diseases [1]. Pain is the most common inflammatory symptom, and the two severe forms of inflammatory pain are osteoarthritis and rheumatoid arthritis [2]. Thus, steroidal or nonsteroidal chemical therapies are the current treatment for inflammatory disorders. Nonsteroidal anti-inflammatory drugs (NSAIDs) are the most commonly used drugs to relieve pain, inflammation, and fever by inhibiting the enzyme cyclooxygenase (COX) [3]. It is well known that the COX enzyme has two isoforms, COX-1 and COX-2. The COX-1 isoform is mainly involved in prostaglandin (PG) biosynthesis in the stomach and provides cytoprotection to the gastric mucosa. The other isoform, COX-2, is inducible and plays a major role in PG biosynthesis in inflammatory cells [4].

Benzimidazole is one of the privileged structures in therapeutic chemistry that acts on different targets to elicit diverse biological activities [5]. The presence of this nucleus in many classes of therapeutic agents such as antimicrobials [6]-[8], antiparasitics [9], anticancers [10], anti-inflammatories, antioxidants, antihypertensives, antidiabetics, as well as antidepressants [11], has made it an indispensable anchor point for the development of new therapeutic agents [12].

Furthermore, the study of metal complexes for pharmacological purposes is based on the intrinsic ability of certain metal ions to modulate the cellular processes involved in inflammation and oxidative stress. Among these metals, cobalt(II) and manganese(III) have chemical and biological properties that are particularly interesting for the development of new entities with anti-inflammatory potential [13].

In addition, Co(II) complexes formed with biologically active ligands, particularly Schiff bases, have demonstrated significant antioxidant and anti-inflammatory activity, attributed to their ability to inhibit certain pro-oxidant enzymes such as cyclooxygenase (COX) and lipoxygenase (LOX) [14]. Mn(III) complexes derived from Schiff bases have also been shown to reduce the release of pro-inflammatory cytokines (such as TNF α and IL 1 β) and decrease lipid peroxidation, demonstrating anti-inflammatory activity linked to the regulation of redox metabolism [15]. Thus, these two metals represent interesting models for the design of new metallopharmaceutical molecules capable of selectively modulating the oxidative and inflammatory mechanisms associated with various chronic diseases.

The aim of this study was to synthesize, characterize, and evaluate the anti-inflammatory properties of two transition metal complexes, Co(II) and Mn(III), obtained from the ligand (2-(1H-benzo[d]imidazol-2-yl)phenol).

2. Materials and Methods

2.1. Reagents and Apparatus

All reagents used were of analytical purity and were used directly without further treatment. Salicylaldehyde, 1,2-diaminobenzene, NH₄SCN, Co(NO₃)₂·6 H₂O,

MnCl₂·4H₂O and croton oil were obtained from Sigma Aldrich. Infrared spectra were obtained on a Perkin Elmer Spectrum Two FTIR spectrometer in the region 4000 - 400 cm⁻¹. The UV-Visible spectrum was recorded on a Perkin Elmer Lambda UV-Vis spectrophotometer. ¹H and ¹³C NMR spectra were recorded in deuterated acetone on a Bruker 500 MHz spectrometer at room temperature using TMS as an internal reference.

2.2. Animal Material

Male mice weighing between 18 - 25 g were provided by the Pasteur Institute of Dakar. They were acclimatized to the laboratory for 7 days prior to the experiment. The animals were housed in cages under conditions of 25°C ± 2°C, with a 12 h light cycle, and provided with food and water ad libitum.

The experimental protocols were conducted in accordance with the guidelines on the care and use of laboratory animals (12/11/2015) by the Research Ethics Committee of Cheikh Anta DIOP University of Dakar (approval no. 0136/2015/CER/UCAD).

2.3. Methods

2.3.1. Synthesis of the Ligand (2-(1H-Benzo[d]imidazol-2-Yl)phenol)

In a 250 mL flask containing 15 mL of ethanol, 3.24 g (30 mmol) of orthophenyldiamine was introduced. After stirring until complete dissolution, 2.42 g of salicylaldehyde were added to a graduated ampoule. Then, the salicylaldehyde solution was added dropwise. An orange solution was formed, which was heated to reflux for 3 hours. The solution obtained was evaporated to dryness in a rotavapor and then cooled in the refrigerator for 24 hours. Yellow crystals were obtained and recovered by filtration. Yield: 75.86%; Tf: 262°C; IR (cm⁻¹): [ν(C=N), 1605], [ν(C-O): 1278], [ν(OH): 3431], [ν(NH): 3344], [ν(C=C)_{ar}: 1528; 1460; 1489]; ¹H NMR (300 MHz, Acetone, δ in ppm): 7.85 (-NH), 7.82 (-OH), 6.91 - 7.51 (m, 8H, H_{ar}); ¹³C NMR (75 MHz, Acetone, δ in ppm): 205.93 (C-11), 159.79 (C-8), 152.88 (C-4 and C-5), 132.56 (C-13 and C-15), 126.52 (C-1 and C-2), 123.86 (C-14), 119.82 (C-3 and C-12), 118.28 (C-6), 113.48 (C-10).

2.3.2. Synthesis of the Complexes

In a flask containing ethanol, 0.053 g (0.25 mmol) of the ligand was successively introduced, as well as the filtrate of the reaction product between (0.25 mmol) of the metal salt and (0.038 g; 0.5 mmol) of NH₄SCN previously solubilized with ethanol and a few drops of water. After stirring for 1 hour, the solution obtained was filtered and then placed in a slow evaporation. Purple and black crystals were obtained for the cobalt and manganese complexes, respectively.

2.3.3. Evaluation of the Anti-Inflammatory Activity

Anti-inflammatory activity was assessed using the analytical method derived from Tubaro [16]. This consists of using the products tested to inhibit edema caused by the local application of an alcoholic solution of croton oil to the ears of mice. Prior

to the experiment, mice were divided into 5 groups of 4 each, weighed, labeled, and fasted for 12 hours with water *ad libitum*.

The so-called “simultaneous” (curative) method, in which the croton oil and anti-inflammatory extract were applied at the same time, was used. Mice in the control group were treated locally on the right ear with 10 μl of an alcoholic solution of 1% croton oil. For mice in the treated groups, 10 μl of the alcoholic solution of 1% croton oil and 10 μl of the test product were applied to the left ear. On the right ear, only 10 μl of the product to be tested was applied.

After 6 hours, the mice were anesthetized with ethyl ether. Their ears were then immediately cut along the cartilage, weighed with a precision balance, and the mice were subsequently sacrificed.

The evaluation of the edema induced was calculated according to the percentage increase in the weight of the right ear (% Incr RE), which expresses the intensity of the inflammation according to the following formula:

$$\% \text{ Incr RE} = \frac{\text{Weight RE} - \text{Weight LE}}{\text{Weight RE}} \times 100$$

RE = right ear

LE = left ear

The anti-inflammatory activity of the products tested was assessed by calculating the percentage of edema inhibition (% Inh) compared to the control batch according to the following formula:

$$\% \text{ Inh} = \frac{\% \text{ Incr control} - \% \text{ Incr treated}}{\% \text{ Incr control}} \times 100$$

2.4. Statistical Analyses

Results were expressed as mean \pm standard error of the mean (SEM). Statistical significance was determined by analysis of variance (ANOVA) followed by Student's t-test, with a significant difference of p-value < 0.05 (n = 4 represents the number of animals in each group).

3. Results and Discussion

3.1. General Study

The IR spectrum of the ligand showed an intense band at 3431 cm^{-1} , attributed to the phenolic $\nu(\text{O-H})$ vibration band [17]. A band located at 1278 cm^{-1} , attributed to the phenolic $\nu(\text{C-O})$ vibration band, was also noted. The band observed at 3344 cm^{-1} is attributed to the $\nu(\text{N-H})$ vibration of the ligand [18]. The phenolic $\nu(\text{C=N})$ and $\nu(\text{C-O})$ vibration bands at 1610 cm^{-1} and 1278 cm^{-1} on the spectrum of the free ligand were observed at lower frequencies on the IR spectra of the cobalt and manganese complexes, respectively, at 1600 and 1259 cm^{-1} and 1602 and 1236 cm^{-1} . The lowering of these frequencies shows the participation of the phenolate oxygen and the azomethine nitrogen atom in the coordination of the metal ions. In addition, the IR spectra of the complexes each reveal the presence of two bands,

which appear in the intervals of [2071 - 2087] and [741 - 746] cm^{-1} . They are respectively attributed to the $\nu(\text{C}\equiv\text{N})$ vibration band and the $\delta(\text{C-S})$ deformation band of a thiocyanate ion (SCN^-) coordinated to the metal centers via the nitrogen atom [19]-[21].

The proton NMR spectrum of the ligand recorded in acetone showed two singlet signals at 7.82 and 7.85 ppm assigned to the phenolic O-H and nitrogen N-H protons, respectively. The signals emerging between 6.91 and 7.51 ppm were assigned to the aromatic protons [22]. The ^{13}C NMR spectrum of the compound showed, despite the solvent signal located at 29.82 ppm, nine other signals corresponding to the different carbon atoms.

Conductometric measurements of freshly prepared millimolar solutions of the complexes were carried out in dimethylformamide (DMF). The results of the conductivity measurements indicate values which, according to Geary [23], are those of neutral electrolytes.

The electronic spectra of the complexes were recorded in DMF at room temperature in the range 200 - 800 nm. The electronic spectrum of the cobalt complex exhibits a low-energy absorption band at 595 nm, attributable to the $d \rightarrow d$ transitions expected for a cobalt(II) ion in an octahedral geometry. In the high-energy region, the complex exhibits intense absorption bands around 327 - 363 nm, corresponding to the $\pi-\pi^*$ and $n \rightarrow \pi^*$ transitions, and a band around 378 nm, attributed to the charge transfer transition from the coordinated ligand to the cobalt(II) centers [24]. The magnetic moment value of 4.75 μB , higher than the theoretical value expected for three unpaired electrons (3.87 μB), is close to that reported by Banerjee [25] for a dinuclear cobalt complex in the same environment. The UV-visible spectrum of the manganese complex contains characteristic ligand and transition bands of the Mn(III) ion. The intense absorption bands at about 328 and 345 nm can be attributed to intra-ligand $\pi \rightarrow \pi^*$ and $n \rightarrow \pi^*$ transitions in the complex. The weak absorption band appearing at 512 nm is attributed to $d \rightarrow d$ transitions. The room temperature magnetic moment of the studied complex is 5.2 μB . This value is close to the reported values expected for high-spin Mn^{3+} ion complexes with octahedral geometry and d^4 configuration, *i.e.*, 4.80 - 5.00 μB . This value is consistent with the oxidation of Mn^{2+} to Mn^{3+} and the presence of the two Mn ions confirmed by X-ray diffraction [26] [27].

3.2. Crystallographic Study

3.2.1. Description of the Crystal Structure of the Ligand

The crystal structure of the ligand was determined by X-ray diffraction. The compound crystallizes in the monoclinic system with the space group $\text{P2}_1/\text{c}$. The unit cell parameters are: $a = 16.864$ (2) \AA , $b = 4.7347$ (4) \AA , $c = 12.9458$ (11) \AA , $\beta = 91.150^\circ$, and $V = 1009.61$ (18) \AA^3 . The asymmetric unit, whose ORTEP scheme is shown in **Figure 1**, consists of a single molecule of the ligand.

The lengths of the C1—N1 and C1—N2 bonds are 1.327 \AA and 1.371 \AA . They correspond to a double and single bond, respectively. The intramolecular hydro-

gen bond O1—H1...N1 reinforces the stability of the structure in the crystal lattice, while the cohesion is ensured by the intermolecular hydrogen bonds N2—H2...O1 (Figure 2).

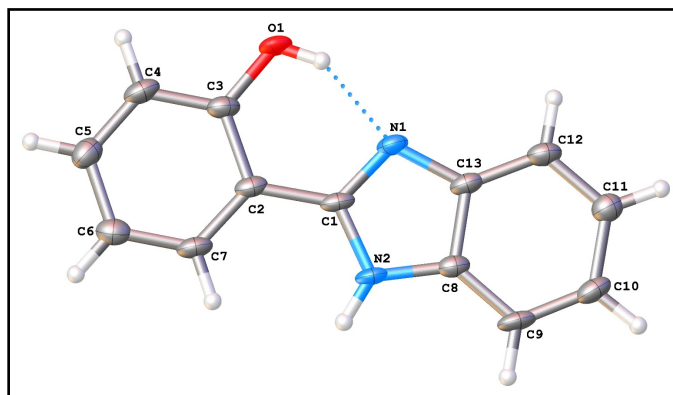


Figure 1. ORTEP view of the ligand.

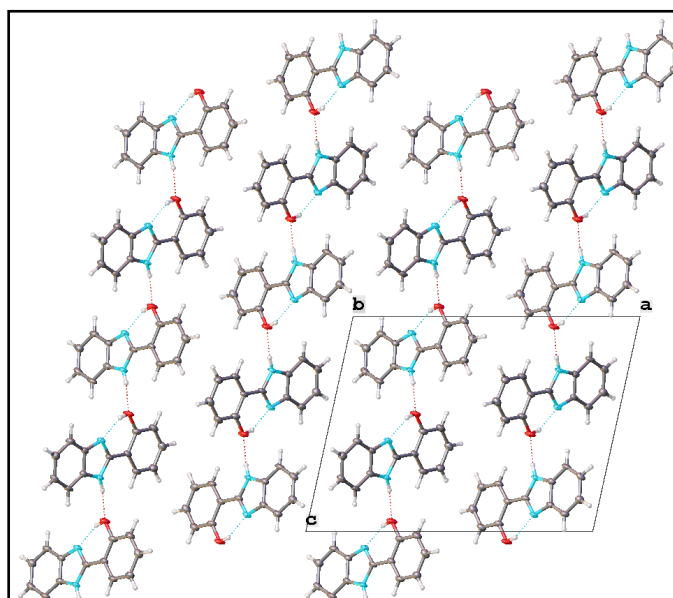


Figure 2. Supramolecular structure of the ligand along the b axis.

3.2.2. Description of the Crystal Structure of the Cobalt Complex

The complex crystallizes in the monoclinic system with the space group $P2_1/c$. The asymmetric unit is composed of a discrete dinuclear complex μ_2 oxo-bridged of Co(II) ions [Co...Co = 3.1326 (6) Å]. Each metal center being pentacoordinated, the geometry is determined using the trigonality parameter τ or Addison index [28] given by $\tau = (\beta - \alpha)/60$ where α and β are the largest values of the bond angles around the central atom. Since the τ values are 0 for a perfect square pyramidal geometry and 1 for a perfect trigonal bipyramidal geometry, the τ value of 0.82 indicates a distorted trigonal bipyramidal geometry around each Co(II). The equatorial plane around the Co ion consists of an azomethine nitrogen atom (N1), the two bridging phenox oxygen atoms (O1), and the nitrogen atom of the thio-

cyanate ion (N3). The sum of the angles subtended by the atom in the equatorial plane is 387.24° . The apical position is occupied by the oxygen atom of the ethanol molecule. The distances in the equatorial plane are 2.0509 (15) Å (Co1—N1), 2.0002 (17) Å (Co1—N3), 1.9612 (13) Å (Co1—O1) and 2.0527 (14) Å (Co1—O2), while that of the axial position is 2.1159 (13) Å (Co1—O1ⁱ). The latter being longer than those in the equatorial plane, this can be explained by a distortion of the Co1—O1ⁱ bond due to the Jahn-Teller effect [29]. The coordination spheres of the two metal centers, symmetrical by an inversion center, include a thiocyanate ion SCN⁻, a solvent molecule (EtOH), and a ligand molecule bridged through its N1 and O1 atoms as shown in **Figure 3**. The C1 crystal packing is directed by a two-dimensional network of N-H...S and O-H...S hydrogen bonds shown in **Figure 4**. These interactions are similar to those reported by Macrae [30].

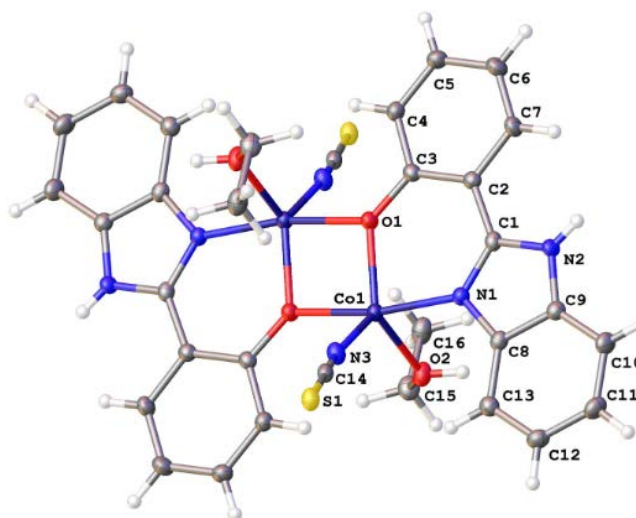


Figure 3. Binuclear complex of Co (II) (ellipsoids represented with a probability of 50%).

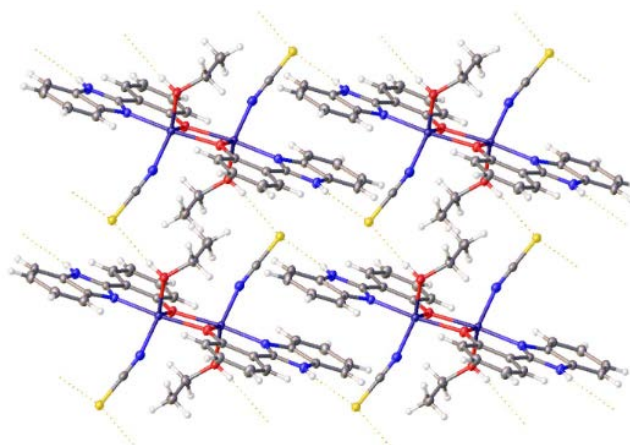


Figure 4. Hydrogen bonds in the cobalt complex (ellipsoids shown with a probability of 50%).

3.2.3. Description of the Crystal Structure of the Manganese Complex

Like the cobalt complex, the manganese complex crystallizes in the monoclinic

system, but in the space group $C2/c$. The asymmetric unit also consists of a discrete dinuclear μ_2 oxo-bridged complex and two free water molecules. The coordination sphere around each Mn(III) is completed by a thiocyanate ion. However, the metal centers have undergone oxidation during formation in air from Mn(II) to Mn(III) [Mn...Mn = 3.3769(7) Å]. The two Mn ions are hexacoordinated and their coordination spheres are related by rotational symmetry. Each M(III) coordinates to an SCN⁻ ion and to two ligands, one via atoms N1 and O1 (bridging) and the other via atoms N3 and O2 (Figure 5).

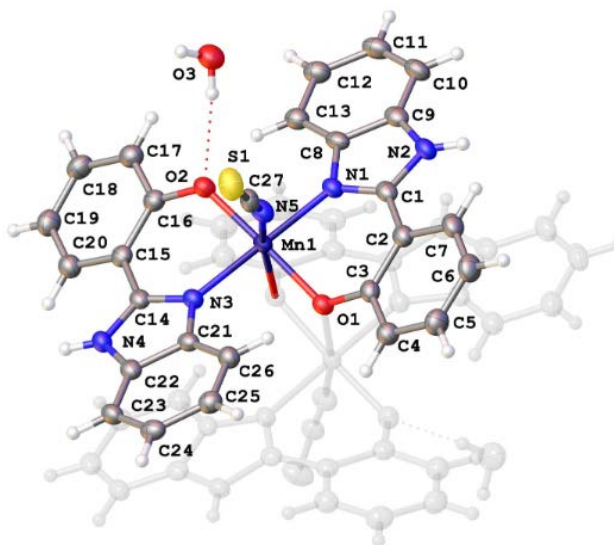


Figure 5. Binuclear complex of Mn(III) (ellipsoids represented with a probability of 50%).

In each monomer, each molecule of the organic ligand is coordinated to the Mn(III) ion by its phenolate oxygen atom and the nitrogen atom of the azomethine function. The coordination sphere around the Mn(III) ion is completed by a thiocyanate SCN⁻ ion and another phenolate oxygen atom from one of the ligands of the other mononuclear unit. The geometry around the Mn(III) ions can thus be described as a distorted octahedron. The phenolate oxygen atoms and the two iminic nitrogen atoms from the two organic ligand molecules occupy the basal plane, while the apical positions are occupied by a phenolate oxygen atom from the other mononuclear unit. The cisoid angles are between [87.30 (7)°–93.10 (6)°], and the values of the transoid angles are O1–Mn1–O2 = 172.72 (7)° and N1–Mn1–N3 = 179.23 (8)°, respectively [25]. These angles have undergone a deviation from the valence angles (90 ° and 180 °) for a regular octahedron, thus confirming the deformation of the polyhedron. The interatomic angles around Mn (III) on the equatorial plane are as follows: O1–Mn1–N1 = 87.30° (7); O1–Mn1–N3 = 93.10° (6); O2–Mn1–N1 = 92.70° (7) and O2–Mn1–N2 = 87.43° (7). Their sum of 360.53, very close to 360°, confirms the octahedral geometry. The interatomic distances Mn1–N1 = 2.0251 (18) Å, Mn1–O2 = 1.8898 (17) Å, Mn1–N3 = 2.0099 (17) Å, and Mn1–O1 = 1.9219 (16) Å, located in the basal plane, are shorter than those in the apical position, Mn1–N5 = 2.177 (2) Å and

$\text{Mn1—O1i} = 2.3869 (16) \text{ \AA}$. This elongation of the bond in the apical position and the compression of those in the equatorial position are justified by the Jahn-Teller effect [31]. **Figure 6** highlights the intermolecular hydrogen bonds of types $\text{O3—H3B...S1}^{\text{IV}}$ and $\text{N4—H4A...S1}^{\text{III}}$ within the crystal lattice. The water molecule is interconnected to the monomer by an intermolecular hydrogen bond of type O3—H3A...O2 .

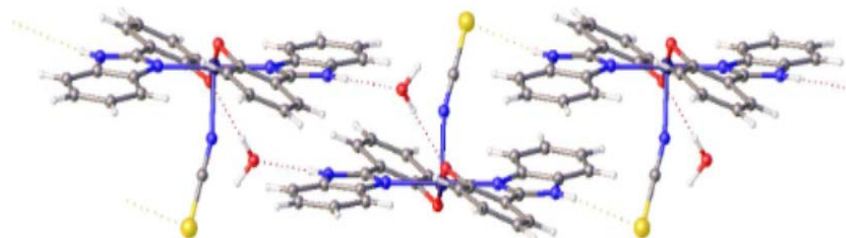


Figure 6. Hydrogen bonds in the Mn(III) complex (ellipsoids shown with a probability of 50%).

3.3. Anti-Inflammatory Activity

The anti-inflammatory activity of the ligand and its complexes was evaluated based on the % Inh of edema in the right ear of croton oil-induced mice. As shown in **Figure 7**, the tested complexes Co(II) and Mn(III) tested at 1% significantly ($p < 0.05$; $p < 0.01$ versus control, respectively) and more strongly inhibited inflammatory ear edema than the 1% free ligand and indomethacin (10%), with % Inh values of 61.26%, 55.48%, 17.03%, and 21.73%, respectively. This suggests that the presence of a central metal improves the specificity of the compounds toward certain biological targets involved in inflammation. Furthermore, the tested ligand showed concentration-dependent anti-inflammatory activity with INH percentages of 17.03 and 52.1% at 1% and 2%, respectively.

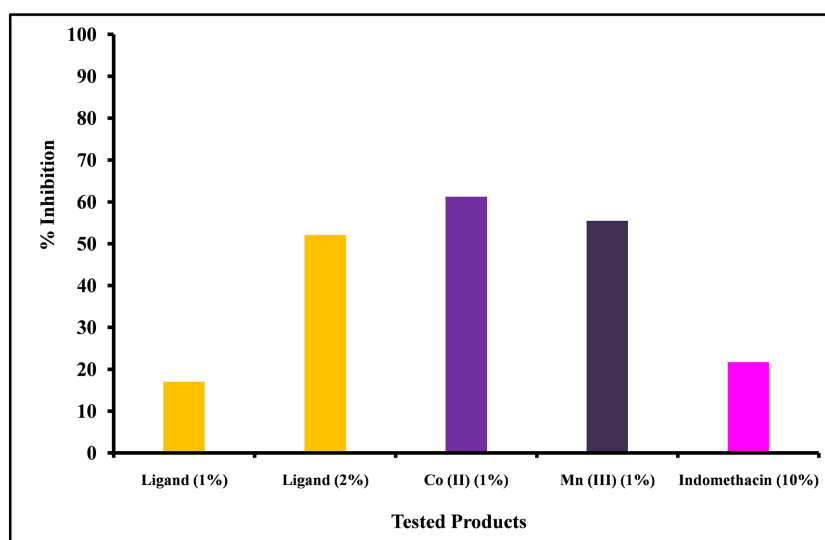


Figure 7. Percentage inhibition of croton oil-induced ear edema after local application of the tested products (free ligand and its complexes and indomethacin).

The Co(II) and Mn(III) metal complexes have high inhibition of edema, suggesting improved biological activity by complexation. The cobalt complex demonstrated superior anti-inflammatory activity compared to the manganese complex. These results suggest that these metal complexes could target specific enzymes or receptors in inflammatory cells and improve therapeutic efficacy.

4. Conclusion

The Schiff base ligand (2-(1H-benzo[d]imidazol-2-yl)phenol) and its two complexes of Co(II) and Mn(III) were synthesized and characterized by different spectroscopic and physical techniques such as NMR, infrared, UV-visible, conductimetry, magnetism, and X-ray diffraction. The XRD results allowed elucidation of the structures of the complexes, where the Mn(III) complex is octahedral and the geometry around Co(II) is a perfect square pyramid. The tests of anti-inflammatory activities of the ligand and its complexes were carried out using the method of mouse ear edema induced by croton oil with indomethacin as a reference. Comparative anti-inflammatory studies have shown that metal complexes exhibit better activity compared to the free ligand and the standard drug. In the near future, it would be necessary to study the anti-inflammatory properties of other transition metal complexes of the same ligand, such as copper and zinc, in order to conclude on other biological properties of this ligand.

Authors' Contributions

This work was carried out in collaboration between all authors. RSG and ND initiated the research theme. RSG, ANS, CD, BF, and MS designed and conducted the study of the anti-inflammatory activity. ND, TEI, and NG designed and conducted the synthesis study. TEI, ND, IN, YT, MB, AD, and ANS analyzed the results. ND wrote the manuscript. ND, RSG, IN, AD, MB, DF, and AW managed the literature search. All authors read and approved the final manuscript.

Acknowledgements

The authors would like to thank the technicians for their help in carrying out this work.

Conflicts of Interest

The authors declare that they have no conflicts of interest.

References

- [1] Badouard, C. (2006) Nucleic Acid Lesions: Detection by HPLC-MS/MS in Human Bio-Logical Environments and Interest as Biomarkers of Oxidative Stress and Inflammation. Doctoral Thesis, Joseph Fourier University, 229 p.
- [2] Gerster, J. (2007) Traitement des arthropathies chondrocalcosiques. *Revue du Rhumatisme*, **74**, 194-198. <https://doi.org/10.1016/j.rhum.2006.11.010>
- [3] Muster, D. (2005) Médicaments de l'inflammation. *EMC—Stomatologie*, **1**, 21-29.

- <https://doi.org/10.1016/j.emcsto.2005.01.005>
- [4] Arora, M., Choudhary, S. and Silakari, O. (2020) *In Silico* Guided Designing of 4-(1H-Benzo[d]Imidazol-2-Yl)phenol-Based Mutual-Prodrugs of Nsaids: Synthesis and Biological Evaluation. *SAR and QSAR in Environmental Research*, **31**, 761-784. <https://doi.org/10.1080/1062936x.2020.1810117>
- [5] Bansal, Y. and Silakari, O. (2012) The Therapeutic Journey of Benzimidazoles: A Review. *Bioorganic & Medicinal Chemistry*, **20**, 6208-6236. <https://doi.org/10.1016/j.bmc.2012.09.013>
- [6] Küçükbay, H. and Durmaz, B. (1997) Antifungal Activity of Organic and Organometallic Derivatives of Benzimidazole and Benzothiazole. *Arzneimittelforschung*, **47**, 667-670.
- [7] Saber, A. and Sebbar, N.K. (2019) Synthesis, Reactivities and Biological Properties of Benzimidazole Derivatives. *Moroccan Journal of Heterocyclic Chemistry*, **18**, 1-50.
- [8] Gavisiddegowda, P., Kollur, S.P., Syed, I. and Revanasiddappa. H.D. (2020) Novel Benzimidazole Derived Imine-Based Ligand and Its Co(III), Ni(II), Cu(II) and Pt(II) Complexes: Chemical Synthesis, Structure, Antimicrobial, DNA Interaction Studies and Nuclease Activity. *Letters in Applied NanoBioScience*, **9**, 1655-1672.
- [9] Ansar, M., Zellou, A., Faouzi, M.E.A., Zahidi, A., Serroukh, S., Lmimouni, B.E., et al. (2009) Synthèse, étude chimique et toxicologique d'un nouveau dérivé benzimidazole. *Annales Pharmaceutiques Françaises*, **67**, 78-83. <https://doi.org/10.1016/j.pharma.2008.11.001>
- [10] Dupuy, M. (2020) Synthesis, Structure and Study of the Antitumor Activity of Original Derivatives of Pyrido[1,2-a] Benzimidazoles. Thèse de doctorat, Université de Montpellier I. <https://theses.fr/2000MON13524>
- [11] Guerret, P. and Langlois, M. (1979) Nouveaux dérivés tricycliques du benzimidazole. *Journal of Heterocyclic Chemistry*, **16**, 1163-1168. <https://doi.org/10.1002/jhet.5570160615>
- [12] Li, Y., Zhang, J., Xie, H., Ge, Y., Wang, K., Song, Z., et al. (2021) Discovery of New 2-Phenyl-1H-Benzo[d]Imidazole Core-Based Potent A-Glucosidase Inhibitors: Synthesis, Kinetic Study, Molecular Docking, and in Vivo Anti-Hyperglycemic Evaluation. *Bioorganic Chemistry*, **117**, Article ID: 105423. <https://doi.org/10.1016/j.bioorg.2021.105423>
- [13] Hernández-Morales, A., Rivera, J.M., López-Monteon, A., Lagunes-Castro, S., Castillo-Blum, S., Cureño-Hernández, K., et al. (2019) Complexes Containing Benzimidazolyl-Phenol Ligands and Ln(III) Ions: Synthesis, Spectroscopic Studies and Preliminary Cytotoxicity Evaluation. *Journal of Inorganic Biochemistry*, **201**, Article ID: 110842. <https://doi.org/10.1016/j.jinorgbio.2019.110842>
- [14] Munteanu, C.R. and Suntharalingam, K. (2015) Advances in Cobalt Complexes as Anticancer Agents. *Dalton Transactions*, **44**, 13796-13808. <https://doi.org/10.1039/c5dt02101d>
- [15] Belkhalifa, H. and Mebarkia, C. (2022) Synthèse, caractérisation et application biologique des complexes de cuivre et de manganèse. Master's Thesis, Université Kasdi Merbah Ouargla.
- [16] Tubaro, A., Dri, P., Delbello, G., Zilli, C. and Loggia, R.D. (1986) The Croton Oil Ear Test Revisited. *Agents and Actions*, **17**, 347-349. <https://doi.org/10.1007/bf01982641>
- [17] Dutta, A.K., Samanta, S., Dutta, S., Lucas, C.R., Dawe, L.N., Biswas, P., et al. (2016) Iron(III) Complexes of 2-(1H-Benzo[d]Imidazol-2-Yl)Phenol and Acetate or Nitrate as Catalysts for Epoxidation of Olefins with Hydrogen Peroxide. *Journal of Molecular*

- Structure*, **1115**, 207-213. <https://doi.org/10.1016/j.molstruc.2016.02.101>
- [18] Yarkandi, N.H., El-Ghamry, H.A. and Gaber, M. (2017) Synthesis, Spectroscopic and DNA Binding Ability of Co^{II}, Ni^{II}, Cu^{II} and Zn^{II} Complexes of Schiff Base Ligand (E)-1-(((1h-Benzo[d]imidazol-2-Yl)methylimino)methyl)naphthalen-2-ol. X-Ray Crystal Structure Determination of Cobalt (II) Complex. *Materials Science and Engineering: C*, **75**, 1059-1067. <https://doi.org/10.1016/j.msec.2017.02.171>
- [19] Mautner, F.A., Louka, F.R., LeGuet, T. and Massoud, S.S. (2009) Pseudohalide Copper(II) Complexes Derived from Polypyridyl Ligands: Synthesis and Characterization. *Journal of Molecular Structure*, **919**, 196-203. <https://doi.org/10.1016/j.molstruc.2008.09.015>
- [20] Bhaumik, P.K., Harms, K. and Chattopadhyay, S. (2013) Synthesis and Characterization of Four Dicyanamide Bridged Copper(II) Complexes with N₂O Donor Tridentate Schiff Bases as Blocking Ligands. *Inorganica Chimica Acta*, **405**, 400-409. <https://doi.org/10.1016/j.ica.2013.06.025>
- [21] Sarr, M., Diop, M., Thiam, I.E., Gaye, M., Barry, A.H., Alvarez, N., et al. (2018) Co-crystal Structure of a Dinuclear (Zn-Y) and a Trinuclear (Zn-Y-Zn) Complexes Derived from a Schiff Base Ligand. *European Journal of Chemistry*, **9**, 67-73. <https://doi.org/10.5155/eurjchem.9.2.67-73.1688>
- [22] Al-Adilee, K. and Dakheel, H. (2018) Synthesis, Spectral and Biological Studies of Ni(II), Pd(II), and Pt(IV) Complexes with New Heterocyclic Ligand Derived from Azo-Schiff Bases Dye. *Eurasian Journal of Analytical Chemistry*, **13**, em64. <https://doi.org/10.29333/ejac/97267>
- [23] Geary, W.J. (1971) The Use of Conductivity Measurements in Organic Solvents for the Characterisation of Coordination Compounds. *Coordination Chemistry Reviews*, **7**, 81-122. [https://doi.org/10.1016/s0010-8545\(00\)80009-0](https://doi.org/10.1016/s0010-8545(00)80009-0)
- [24] Ghosh, K., Roy, S., Ghosh, A., Banerjee, A., Bauzá, A., Frontera, A., et al. (2016) Three Mononuclear Octahedral Cobalt(III) Complexes with Salicylaldehyde Schiff Bases: Synthesis, Characterization, Phenoxazinone Synthase Mimicking Activity and DFT Study on Supramolecular Interactions. *Polyhedron*, **112**, 6-17. <https://doi.org/10.1016/j.poly.2016.02.035>
- [25] Banerjee, A., Herrero, S., Gutiérrez, Á. and Chattopadhyay, S. (2020) Synthesis, Structure and Magnetic Property of a Dinuclear Cobalt(II/III) Complex with a Reduced Schiff Base Ligand. *Polyhedron*, **190**, Article ID: 114756. <https://doi.org/10.1016/j.poly.2020.114756>
- [26] Bartyzel, A. (2013) Synthesis, Crystal Structure and Characterization of Manganese(III) Complex Containing a Tetradentate Schiff Base. *Journal of Coordination Chemistry*, **66**, 4292-4303. <https://doi.org/10.1080/00958972.2013.867029>
- [27] Orton, J.B., Diouf, N., Gueye, R.S., Gaye, M., Thiam, I.E. and Coles, S.J. (2023) Synthesis and Crystal Structures of Two Related Co and Mn Complexes: A Celebration of Collaboration between the Universities of Dakar and Southampton. *Acta Crystallographica Section E Crystallographic Communications*, **79**, 1109-1114. <https://doi.org/10.1107/s2056989023009805>
- [28] Addison, A.W., Rao, T.N., Reedijk, J., van Rijn, J. and Verschoor, G.C. (1984) Synthesis, Structure, and Spectroscopic Properties of Copper(II) Compounds Containing Nitrogen-Sulphur Donor Ligands; the Crystal and Molecular Structure of Aqua[1,7-Bis(N-Methylbenzimidazol-2'-yl)-2,6-Dithiaheptane]Copper(II) Perchlorate. *Journal of the Chemical Society, Dalton Transactions*, **7**, 1349-1356. <https://doi.org/10.1039/dt9840001349>
- [29] Thakurta, S., Butcher, R.J., Gómez-García, C.J., Garribba, E. and Mitra, S. (2010) Syn-

- thesis, Structural Aspects and Magnetic Properties of an Unusual 2D Thiocyanato-Bridged Cobalt(II)-Schiff Base Network. *Inorganica Chimica Acta*, **363**, 3981-3986. <https://doi.org/10.1016/j.ica.2010.07.069>
- [30] Macrae, C.F., Sovago, I., Cottrell, S.J., Galek, P.T.A., McCabe, P., Pidcock, E., *et al.* (2020) Mercury 4.0: From Visualization to Analysis, Design and Prediction. *Journal of Applied Crystallography*, **53**, 226-235. <https://doi.org/10.1107/s1600576719014092>
- [31] Diouf, N., Thiam, I.E., Sylla-Gueye, R., Retailleau, P. and Gaye, M. (2022) Syntheses, Characterization, and X-Ray Crystal Structure of a Co-Crystal Containing One Neutral Mononuclear Copper (II) Unit and One Cationic Dinuclear Copper (II) Unit Assembled with Schiff Base and Perchlorate Copper(II) Salt. *Earthline Journal of Chemical Sciences*, **8**, 35-52. <https://doi.org/10.34198/ejcs.8122.3552>